Integral Theory for the Instability of Laminar Compressible Wakes behind Slender Bodies

DENNY R. S. KO*
TRW Systems Group, Redondo Beach, Calif.

An integral theory is developed for studying the instability of laminar compressible wakes behind slender bodies. The mean flow is assumed to be characterized by a few shape parameters and a Gaussian distribution. Distribution of the fluctuations across the wake is obtained as a function of these mean flow parameters by solving the inviscid linearized fluctuation equations using the local mean flow. The fluctuation field is coupled with the mean flow through the Reynolds stress term, and the variation of the fluctuation amplitude is then obtained, together with the mean flow parameters, by solving the integral conservation equations. Both axisymmetric and planar bodies are considered, and favorable comparison with available two-dimensional experimental results is indicated.

I. Introduction

BECAUSE of the inherited dynamical instability associated with its mean profiles, a laminar wake at high Reynolds number is generally unstable, and transition to a turbulent wake commences under most circumstances. Most of our present understanding of the transition from a laminar to a turbulent wake has relied on experimental observations. On the other hand, relatively meager analytical effort has not been able to provide a deeper understanding of the transitional process. The first clue for the breakdown of a laminar wake was furnished by classical linear stability theory, which showed that a laminar wake is unstable to a wide range of infinitesimal disturbances. The existence of such a linearly unstable region has also been well demonstrated in various wake experiments, e.g., Sato and Kuriki's experiment[1] for a two-dimensional incompressible wake, Sato and Okada's experiment[2] for an axisymmetric incompressible wake, and Behrens and Ko's[3] experiments for a two-dimensional compressible wake. However, the linearized theory is valid only over a fairly limited region in a wake because of its inherent small-amplitude approximation.

In an effort to extend the region of validity for the theoretical approach, Stuart[4] and Watson[5,6] formulated a nonlinear stability theory for an incompressible parallel flow. Reasonable agreement has been obtained between their theory and the experiment of Taylor[7] for the case of circular Couette flow. An attempt to extend this theory to a two-dimensional compressible wake was reported by Liu.[8] The approach is based on the hypothesis of a small linear amplification rate, which results in a weak interaction between the disturbance and the mean flowfield. Therefore, the deviation of the mean flowfield from a laminar state can be considered as small and represented by a power series in the amplitude of the fluctuation. However, because of the unstable nature of the wake, such a small deviation from the laminar state is not realized much beyond the linearly unstable region in most practical situations. Additional complication is caused by the growth of the wake which further restricts the range of validity of the parallel flow approach. Ko[9] has suggested a cascade method of solution for a nearly parallel incompressible wake flow by supplementing the theory of Stuart and Watson with an integral approach. The use of an approximate integral approach has relaxed the relatively strong limitation of a small linear amplification rate required in the theory of Stuart and Watson. The success of such an approach is indicated in the first-order results of Ko et al.,[10] where the stability of a laminar incompressible wake behind a flat plate was considered. Over-all agreement with the experiments of Sato and Kuriki has demonstrated the adequacy of such a model for describing the breakdown of a laminar incompressible wake.

A large number of experiments for studying the transitional processes in a compressible wake have been reported in recent years. Close similarity in the transitional processes between the compressible and incompressible wakes has been observed (e.g., Behrens and Ko[3]). It is the objective of the present investigation to apply a similar integral approach to study the transition phenomenon in a compressible wake. Both axisymmetric and two-dimensional wakes are considered in this study.

Received October 13, 1970; revision received March 31, 1971. This work was supported by Bell Telephone Laboratories Inc. under the Reentry Measurements Instrumentation Package Program, Contract 601561.

Index Categories: Boundary-Layer Stability and Transition; Supersonic and Hypersonic Flow; Jets, Wakes, and Viscous-Inviscid Flow Interaction.

* Staff Engineer, Engineering Technology Department, Fluid Mechanics Laboratory.

II. Formulation

2.1. General Assumptions

In order to simplify the analysis while still retaining the essential features of the transition process, the following assumptions are introduced: 1) constant wake edge conditions, 2) constant momentum deficit in the wake, 3) high Reynolds number flow, and 4) ideal gas and no chemical reaction. The first two assumptions amount to a negligible outer inviscid wake, which, in reality, limits the present analysis to slender bodies with relatively sharp leading edges. The high Reynolds number assumption is generally valid for most flows of practical interest and permits a boundary-layer approximation to the mean flow. If necessary, most of these assumptions can be relaxed easily in the analysis with no conceptual difficulty to allow for a more complete description of the flow.

Each flow variable is decomposed into a mean steady component and a fluctuating component, e.g.,

$$\mathbf{u} = \langle \mathbf{u}(\mathbf{x}) \rangle + \mathbf{u}'(\mathbf{x},t) \tag{1}$$

with

$$\langle \mathbf{u}' \rangle = 0 \tag{2}$$

where the angular bracket is used to represent a time average

over a suitably chosen period, whereas boldface type indicates a vector. The full Navier-Stokes equation for a viscous compressible fluid can then be separated easily into a set for the mean and a set for the fluctuating components.

2.2. Method of Approach

In the transition region, the fluctuating component is expected to have a finite amplitude, which precludes the usual decoupled treatment of linear stability theory. Therefore, the mean and the fluctuation fields will have to be considered simultaneously. In principle, the complete set of partial differential equations can be solved for given boundary and initial conditions of any desired flow. However, the complexity of the system makes such an approach impractical within the present computational capability. Therefore, an integral method of solution, which has been applied successfully to the case of an incompressible flat plate wake,[10] will be used for the present investigation. An approximate solution is sought which satisfies the conservation equations in integral form. The essence of an integral approach lies in the proper representation of the complete flowfield by a few parameters. The detail distributions are relatively unimportant if the governing parameters have been carefully chosen with the correct physical background. The basic thinking of the approach is to devise a phenomenological theory for the transitional region. In close analogy to the much explored phenomenological approach to a turbulent flow, the main concern here is the suitable form of the Reynolds stress needed to provide the coupling between the mean and the fluctuation. This information will be obtained in the present approach with the help of the linearized fluctuation equations. The general approach will be described in more detail in the following sections.

2.3. Integral Equations

Let (u,v,w) be the velocity field corresponding to the axisymmetric coordinate system (x,r,θ). [Similarly, let (u,v) correspond to the two-dimensional coordinate system (x,r).] Since only the time-averaged equations will be presented in this section, the angular bracket will be dropped from the nonfluctuating quantities. All equations are presented in nondimensional form, using the edge quantities (e.g., U_e,ρ_e,p_e, and T_e) and a characteristic body dimension L.

The full equations are simplified by invoking the high Reynolds number assumption to the mean flowfield. In the case of an axisymmetric wake, it is further assumed that no swirl is transmitted to the wake. Thus, $\langle w\rangle = 0$, and the mean azimuthal momentum equation can be ignored. To further simplify the analysis, the triple correlation terms are taken to be zero.† After some manipulation, the required integral equations can be obtained in the following form (where $m = 0$ for two-dimensional and $m = 1$ for axisymmetric cases):

Mean Radial Momentum Integral Equation

$$-\frac{1}{\gamma M_e^2}[p(r) - 1] = \rho\langle v'^2\rangle - m\int_r^\infty \rho(\langle v'^2\rangle - \langle w'^2\rangle)\frac{dr}{r} \tag{3}$$

which gives the mean static pressure field.

Mean Axial Momentum Integral Equation

$$\int_0^\infty \left[\rho(u^2 - u) + \rho\langle u'^2\rangle + \langle\rho'u'\rangle(2u - 1) + \frac{p-1}{\gamma M_e^2}\right]\times r^m\,dr = \frac{C_D}{4\pi^m} \tag{4}$$

where C_D = (drag of the inner wake)/$\frac{1}{2}\rho_e U_e^2 L^{m+1}$ and M_e denotes the edge Mach number.

Mean Thermal Energy Integral Equation

$$\frac{d}{dx}\int_0^\infty [\rho u(T-1) + \langle\rho'u'\rangle(T-1) + \rho\langle u'T'\rangle + u\langle\rho'T'\rangle]r^m\,dr = \frac{\gamma-1}{\gamma}\int_0^\infty\left[v\frac{\partial p}{\partial r} + u\frac{\partial p}{\partial x} + \left\langle u'\frac{\partial p'}{\partial x} + v'\frac{\partial p'}{\partial r} + m\frac{w'}{r}\frac{\partial p'}{\partial\theta}\right\rangle\right]r^m\,dr + \frac{(\gamma-1)M_e^2}{R_e}\left[\int_0^\infty \mu\left(\frac{\partial u}{\partial r}\right)^2 r^m\,dr + \int_0^\infty\langle\phi'\rangle r^m\,dr\right] \tag{5}$$

where ϕ' represents the viscous terms involving the fluctuating components, and $R_e = U_e L/\nu_e$.

Mean Kinetic Energy Integral Equation

$$\frac{d}{dx}\int_0^\infty\left[\tfrac{1}{2}\rho u(u^2-1) + \tfrac{1}{2}\langle\rho'u'\rangle(3u^2-1) + \rho u\langle u'^2\rangle + \frac{(p-1)u}{\gamma M_e^2}\right]r^m\,dr = \int_0^\infty\left[(\rho\langle u'v'\rangle + v\langle\rho'u'\rangle)\frac{\partial u}{\partial r} + \left(\rho\langle u'^2\rangle + u\langle\rho'u'\rangle + \frac{p-1}{\gamma M_e^2}\right)\frac{\partial u}{\partial x}\right]r^m\,dr - \frac{1}{R_e}\int_0^\infty\mu\left(\frac{\partial u}{\partial r}\right)^2 r^m\,dr \tag{6}$$

An additional integral equation to be used in the present analysis is given by the kinetic energy equation for the fluctuating component, which can be easily obtained from the fluctuation equations.

Integrated Fluctuation Energy Equation

$$\frac{d}{dx}\int_0^\infty \rho u E r^m\,dr = -m\int_0^\infty E\frac{\partial}{\partial r}[r\langle\rho'v'\rangle]\,dr - \int_0^\infty\langle\rho'u'\rangle\left(v\frac{\partial u}{\partial r} + u\frac{\partial u}{\partial x}\right)r^m\,dr - \int_0^\infty\rho\left[\langle u'v'\rangle\frac{\partial u}{\partial r} + \langle v'^2\rangle\frac{\partial v}{\partial r} + \langle u'^2\rangle\frac{\partial u}{\partial x} + \frac{mv}{r}\langle w'^2\rangle\right]r^m\,dr - \frac{1}{\gamma M_e^2}\int_0^\infty\left\langle u'\frac{\partial p'}{\partial x} + v'\frac{\partial p'}{\partial r} + m\frac{w'}{r}\frac{\partial p'}{\partial\theta}\right\rangle r^m\,dr - \frac{1}{R_e}\int_0^\infty\langle\phi'\rangle r^m\,dr \tag{7}$$

where $E = \frac{1}{2}[\langle u'^2\rangle + \langle v'^2\rangle + m\langle w'^2\rangle]$.

2.4. Mean Flow Model

There is enough experimental evidence to suggest that the mean flow quantities (velocity and density) have nearly Gaussian distributions across the wake with proper normalization. This is valid throughout the whole wake length except in the immediate vicinity of the body. Therefore, the mean axial velocity field is assumed to be characterized by two parameters in the following form:

$$u(r,x) = 1 - W_c(x)W^*(\eta) \tag{8}$$

where

$$\eta = r/b(x) \qquad W^* = \exp(-k_1\eta^2)$$

and where b is the velocity wake half-width and W_c is the centerline velocity defect, $1 - u(0,x)$. The constant k_1 is set to be 0.693, which defines the characteristic width b as the distance from the axis to the half-velocity defect point. A similar expression is used for the density field, i.e.,

$$\rho(r,x) = 1 - \rho_c(x)D^* \tag{9}$$

† This is actually a consequence of the single frequency model used for the fluctuation field.

where

$$\rho_c = 1 - \rho(0,x) \qquad \text{(the centerline density defect)}$$

and

$$D^* = \exp(-k_2\eta^2)$$

The relative magnitude of k_2 to k_1 indicates the relative size of the density (or temperature) wake to the velocity wake. For simplicity, k_2 is taken to be a constant equal to 0.5 based on a square-root dependence of the Prandtl number with $Pr = 0.72$. The other mean flow quantities can be obtained in terms of ρ,u, and the fluctuation field. For example, the mean static pressure field can be obtained easily from Eq. (3), which gives

$$-(\gamma M_e^2)^{-1}(p - 1) = \rho\langle v'^2\rangle - m\int_\eta^\infty \rho(\langle v'^2\rangle - \langle w'^2\rangle)\frac{d\eta}{\eta} \qquad (10)$$

2.5. Fluctuation Modeling

It is clear from inspecting the integral equations that the fluctuation field should also be characterized by a few parameters. The present approach seeks the simplest yet most reasonable way of representing the fluctuation field with the least number of additional parameters. A natural source from which to obtain information concerning the fluctuations is through their governing differential equations. The approach used in Ref. 9 assumes the dominance of a single frequency fluctuation at the initial stage. A rather formal expansion solution in series of the amplitude is also proposed to account for the nonlinear effects in a "cascaded" manner. This type of spectrum for the fluctuation quite appropriately resembles that of an incompressible wake. In the case of a compressible wake, a much broader spectrum is normally observed. Therefore, the single frequency representation should not be taken literally but should be considered as a means of obtaining the functional dependence of the Reynolds stresses on the flow parameters. Based on the findings of the two-dimensional incompressible wake, the higher-order effects will be neglected in the present calculations. Thus, the nonlinear terms in the fluctuation equation will be ignored. Furthermore, the viscous and heat-conducting terms are neglected based on the study of Lin,[11] which states that the inviscid solution is a close approximation to the exact solution in the case of an amplified disturbance. In addition, the local parallel mean flow assumption is used, i.e., $\langle v\rangle = \langle w\rangle = 0$ and no axial variation of the mean quantities. Then, this set of linearized governing equations for the fluctuation field permits a wave-like solution of the form

$$\left.\begin{aligned} u' &\sim q_x(r)e^{i\Theta} + \text{conjugate}\\ v' &\sim iq_r(r)e^{i\Theta} + \text{conjugate}\\ w' &\sim \text{m } q_\theta(r)e^{i\Theta} + \text{conjugate}\\ \rho' &\sim s(r)e^{i\Theta} + \text{conjugate}\\ p' &\sim \pi(r)e^{i\Theta} + \text{conjugate}\\ T' &\sim \phi(r)e^{i\Theta} + \text{conjugate} \end{aligned}\right\} \qquad (11)$$

with

$$\Theta = \alpha x - \omega t + mn\theta$$

Notice that, in the case of axisymmetric wake, the fluctuation field depends on the azimuthal angle θ, whereas the mean flow is considered to be axially symmetric. Here, the spatial mode of fluctuation is considered, i.e., the fluctuation grows or decays with distance. In other words, in Eq. (11), ω = nondimensional frequency (real), and $\alpha = \alpha_r + i\alpha_i$ (nondimensional complex wave number), with $(-\alpha_i)$ being proportional to the local spatial rate of amplification. n is an integer that will be taken as 1 in the present investigation for axisymmetric case. This choice is based on the temporal study of Lees and Gold,[12] which shows that the $n = 1$ mode (helical mode) provides a much higher amplification rate than the other modes with $n \neq 1$. The antisymmetric mode, $u'(r = 0) = 0$, is chosen for the two-dimensional case for a similar reason.

The derivation of the governing equations and the proper set of boundary conditions have been fully discussed by Lees and Gold[12] and Batchelor and Gill[13] and will not be restated here. For the purpose of numerical computations, it is more convenient to work with a second-order equation for a single variable, say π. The governing equation for the pressure fluctuation π is given by

$$\frac{d}{d\eta}\left[\frac{\eta^m(d\pi/d\eta)}{\bar\rho(W^* - c)^2}\right] - \left[\frac{(mn^2 + \eta^{2m}\alpha^{*2})}{\eta^m\bar\rho(W^* - c)^2} - \eta^m\alpha^{*2}M^2\right]\pi = 0 \qquad (12)$$

where

$$\begin{aligned} c &= (W_c)^{-1}[1 - (\omega b/\alpha^*)]\\ \alpha^* &= \alpha b, \qquad M = M_e W_c \end{aligned} \qquad (13)$$

The other quantities can be easily deduced from π and its derivatives. The corresponding boundary conditions for Eq. (12) are

$$\left.\begin{aligned} \eta = 0 \qquad & \pi = 0 && \text{(for } n \neq 0 \text{ in axisymmetric case)}\\ \eta \to \infty \qquad & \pi \sim K_n(\beta\eta) && \text{(axisymmetric)}\\ & \pi \sim e^{-\beta\eta} && \text{(two-dimensional)} \end{aligned}\right\} \qquad (14)$$

where K_n represents modified Bessel function of the second kind of the nth order and

$$\beta = \pm\alpha[1 - M^2c^2]^{1/2} \qquad (14a)$$

The sign of the square root is chosen such that the real part of β is positive. The disturbance is considered as supersonic, sonic, or subsonic, depending on whether the real part of c is greater than, equal to, or less than $(1/M)$.

Equation (12), together with the homogeneous boundary conditions (14), forms an eigenvalue problem. The solutions can be obtained numerically using the linear eigenvalue search method of Mack.[14] In general, the eigenvalue and the eigenfunction have the following functional dependence:

$$\begin{aligned} \alpha^* &= \alpha^*(M_e,\rho_c,W_c,\omega b)\\ \pi &= \pi(\eta;M_e,\rho_c,W_c,\omega b) \end{aligned} \qquad (15)$$

for given k_1 and k_2. The integrals involving the fluctuating components can then be determined as functions of M_e,ρ_c,W_c, and ωb once and for all. To simplify the analysis, the edge Mach number is taken to be a given constant, and the disturbance is assumed to have a constant physical frequency ω. The proper frequency for certain flow conditions is given by the most unstable one calculated from the local mean flow near the origin of the wake, where the flow is presumed to be laminar. One further approximation is then introduced by neglecting the contributions from the fluctuating quantities to the integrated axial momentum equation. Then, the wake half-width b is related to the other two mean flow parameters ρ_c and W_c algebraically. By doing so, the functional dependence appearing in Eq. (15) reduced to two

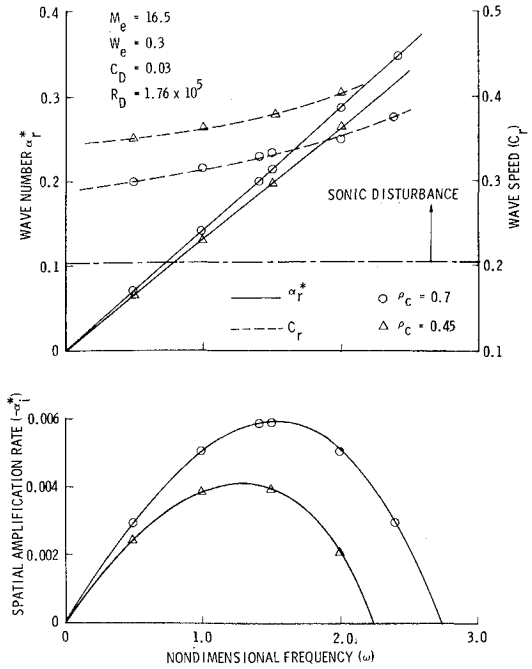

Fig. 1 Eigenvalues for axisymmetric compressible wake.

parameters, ρ_c and W_c. All of the integrals involving the fluctuations can now be expressed as functions of these two parameters. However, since the linearized problem is homogeneous, all integrals are determined up to a constant multiplier, which is taken to be the turbulent energy intensity and will be determined simultaneously with the mean field. For example, the Reynolds stress integral can be written as

$$\int_0^\infty \rho\langle u'v'\rangle\eta^m\, d\eta = A^2 I(\rho_c, W_c) \tag{16}$$

Some of the approximations used to arrive at expression (16) may seem to be weak over the whole transitional region. However, it should be emphasized that the linearized fluctuation equation is used merely as a tool to obtain the proper correlation between the fluctuating quantities and the mean flowfield which is needed in the integral formulation. These correlations are obtained in advance with a limited number of computations covering the ranges of interest. The same information could, in principle, be obtained from a controlled experiment (an alternate but more frequent way of achieving a phenomenological theory). Since the detailed distribution is not of vital importance to an integral method of solution, the present approach is expected to be adequate for a large portion of the transition region. However, there is no provision in the theory to treat a fully developed turbulent wake at the present time. In fact, because of the viscous dissipation effect, the solution will eventually return to a laminar one in the present calculation.

2.6. Initial-Value Problem

Using the proposed models for the mean and the fluctuating fields, the complete problem has been reduced to solving for the four unknown quantities: the velocity wake width b, the wake velocity defect W_c, the centerline density defect ρ_c, and the turbulent intensity A^2. The solutions, as functions of the axial distance behind the body, can be obtained by simultaneous integration of the four integral conservation equations for the momentum, the mean kinetic energy, the mean thermal energy, and the fluctuation energy. The mean momentum integral equation can be integrated readily to provide an algebraic relation between the four unknowns. The remaining integral equations can then be written in the following form:

$$K_{iw}\frac{dW_c}{dx} + K_{id}\frac{d\rho_c}{dx} + K_{ia}\frac{dA^2}{dx} = K_i \tag{17}$$

with K_{iw}, K_{id}, K_{ia}, and K_i being known functions of ρ_c, W_c, and A^2. This set of first-order nonlinear differential equations can be solved numerically as an initial-value problem by starting the integration near the wake neck with appropriate initial values of W_c, ρ_c, and A^2. The initial value of W_c represents essentially the drag of the inner wake. The initial value of ρ_c represents the temperature excess on the wake centerline at the neck which gives the effect of body cooling. The initial value of A^2 gives the turbulent intensity level at the wake neck. The effects on the transitional process of these initial values will have to be studied numerically.

III. Results and Discussions

3.1. Axisymmetric Wake

To demonstrate the transition phenomenon in the wake of an axisymmetric body, the following conditions have been used as a test case:

edge Mach number, $M_e = 16.5$
Reynolds number based on edge conditions, $R_D = 1.76 \times 10^5$
drag coefficient of the inner wake, $C_D = 0.03$

Since the integral equations are solved as an initial-value problem, the following conditions are chosen to be the representative values at the wake neck, which is taken to be the initial station in the present calculations:

$$\left.\begin{aligned}&\text{initial centerline velocity defect } W_{c0} = 0.3\\ &\text{initial centerline density defect } \rho_{c0} = 0.9\\ &\text{initial fluctuation energy level } Z_0 = 10^{-8}\end{aligned}\right\} \tag{18}$$

Here Z, defined as

$$Z = \int_0^\infty E\eta^m\, d\eta$$

represents the integrated fluctuation energy density, which gives a measure of the turbulent intensity in the wake. This initial intensity Z_0 corresponds to an initial velocity fluctuation on the order of 1 fps.

3.1.1. *Linear stability equations*

The modeling for the fluctuation field requires a proper choice of the characteristic frequency to be used for obtaining the integrals. Since the initial amplitude of the fluctuation is expected to be small, the linear stability theory is valid, at

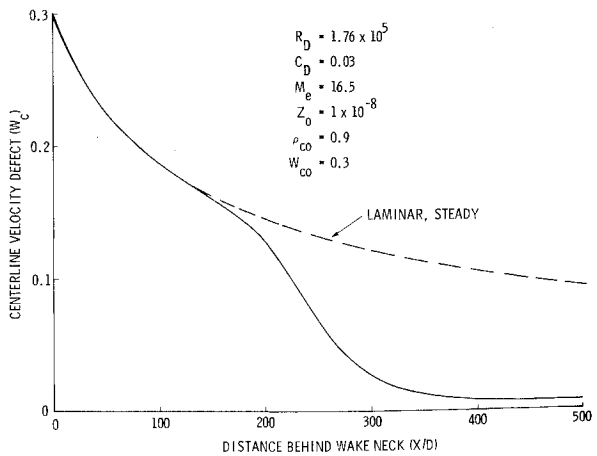

Fig. 2 Variation of the centerline velocity defect.

least in the first portion of the wake transition region. Thus, the characteristic frequency is selected from the solutions of the linear stability equations corresponding to the initial conditions at wake neck. Figure 1 gives the eigenvalues as a function of the nondimensional frequency (nondimensionalized with the edge velocity U_e and base diameter D). The frequency with the maximum spatial amplification rate is chosen to be the characteristic one. As indicated in Fig. 1, a slightly different value may be chosen, depending on the mean flowfield at the initial station. However, the choice of the characteristic value over a fairly wide band of frequencies with compatible local amplification rate is not expected to influence the over-all results to a large extent. The characteristic frequency is chosen to be 1.5 for the present calculation.

A nearly linear dependence of the wave number α_r on the frequency is also shown in Fig. 1. However, because of the nonvanishing imaginary component α_i, the wave speed C_r is not a constant. It may be noted that, at these conditions, most of the amplified modes correspond to the so-called supersonic disturbance. Because of the past misconception on the nonexistence of a supersonic disturbance, it should be emphasized that no particular distinction between a subsonic and a supersonic disturbance is given in the present analysis. In fact, as one follows a given frequency along the wake, the disturbance changes smoothly from a supersonic to a subsonic one. Thus, there is no sudden change in the integrals, which are the main concern in an integral approach.

3.1.2. *Transition phenomenon*

Using the integrals obtained from solving the linear stability equations, the integral equations (17) can be readily integrated numerically using the initial conditions (18). Figure 2 shows the calculated wake velocity defect as a function of the streamwise distance behind the neck. Also shown on the same plot is the velocity decay for a laminar steady wake under the same conditions. The corresponding growth of the wake is shown in Fig. 3. A fairly rapid increase of the size of the wake is seen to accompany the transitional process. The computed centerline density defect is presented in Fig. 4. All three mean flow variables present a similar trend, which may be understood with the help of Fig. 5, where the evolution of the fluctuation energy density Z is shown. For $x/D < 200$, the fluctuation intensity is not high enough to affect the mean flow, and the calculated results follow the laminar curve. Near $x/D = 200$, the defects deviate from the laminar curve and decay at a much faster rate. Finally, the decay rate slows down again, mainly because of the rapid

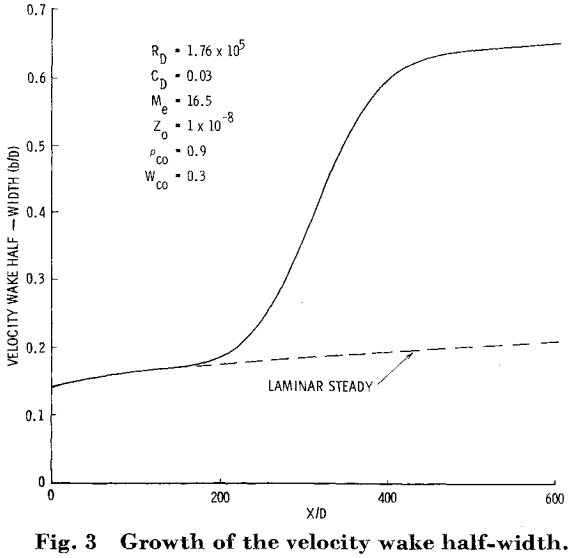

Fig. 3 Growth of the velocity wake half-width.

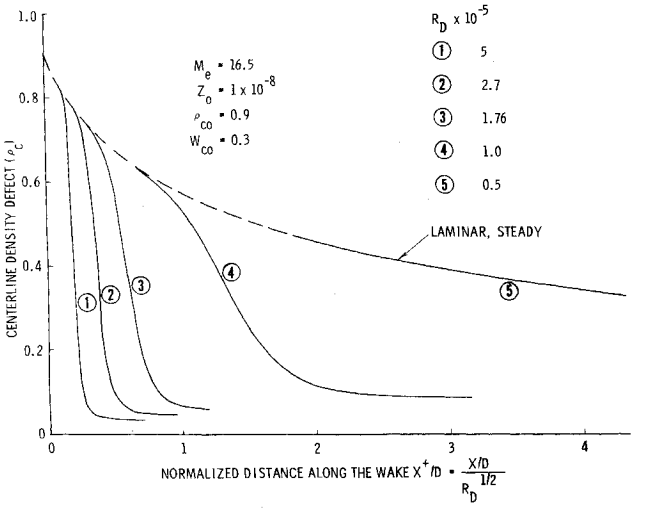

Fig. 4 Reynolds number effect on the centerline density defect.

expansion of the wake, limiting further growth of the fluctuation.

It is appropriate to emphasize that the present model does not provide a proper description of the turbulent wake. Therefore, the solutions become increasingly inadequate for increasing x/D. A generalized analysis, including a patched region to a fully developed turbulent model in existence today (e.g., Lees and Hromas[15]), is needed for a complete description of the flowfield in a wake. However, for the purpose of studying the transitional phenomenon, the present model is believed to be quite adequate. Since we may visualize the single-frequency representation as a first-order effect in a series expansion solution in amplitude A for the fluctuation field, the magnitude of A can be used as a rough measure of the validity of the theoretical model. Based on the criterion of A being less than certain magnitude (say 0.3), the location where such a limit is exceeded in general occurs some distance downstream of the peak of the fluctuation energy density Z. Further studies and comparison with experimental observations are needed before any definitive statement can be made.

3.1.3. *Reynolds number effects*

Using the present theory, the effect of freestream Reynolds number is studied by invoking the following assumptions:

1) Drag coefficient of the inner wake is mainly due to the skin friction of the body and is proportional to $R_D^{-1/2}$.

2) The physical frequency of the characteristic fluctuation mode varies with Reynolds number in such a way that a

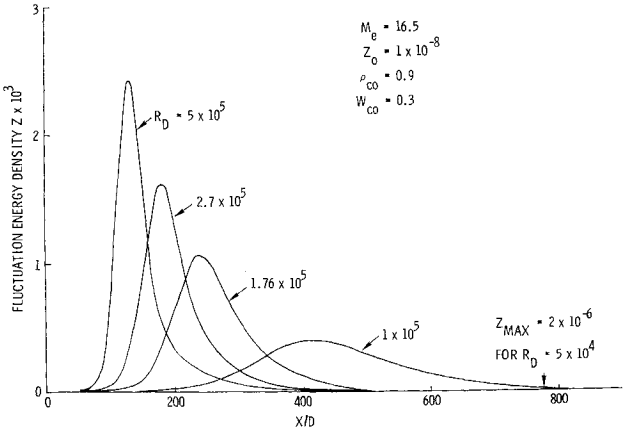

Fig. 5 Reynolds number effect on fluctuation energy density.

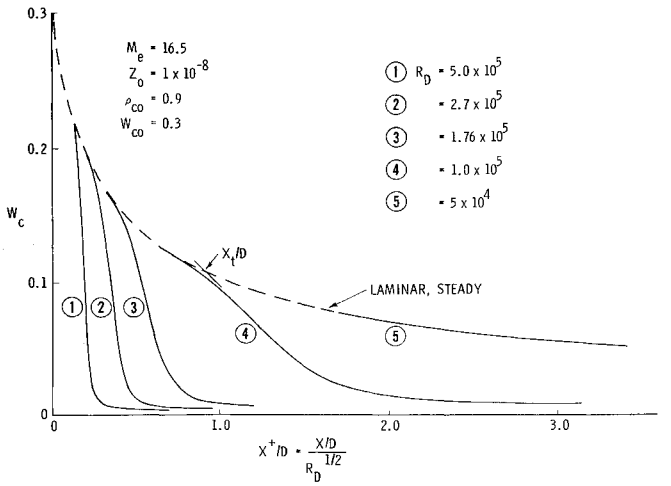

Fig. 6 Reynolds number effect on the centerline velocity defect.

locally normalized frequency ωb remains constant. From Eqs. (15), this assumption implies that the same functional dependence of the integrals on the mean flow parameters W_c and ρ_c can be used for all Reynolds numbers, as long as the other flow conditions remain unchanged.

3) The same initial conditions (18) are used for all calculations in order to single out the Reynolds number effects. In reality, the flow conditions near the wake neck are functions of the Reynolds number, a result to be revealed by studies of the laminar near wake (e.g., Ohrenberger and Baum[16]).

The calculated variations of the fluctuation intensity for various Reynolds number are also shown in Fig. 5. Following each Reynolds number, the fluctuation energy density first grows exponentially as predicted by the linear stability theory, but soon reaches a peak and then decays, caused originally by the rapidly expanding wake and later by the viscous dissipation. It may also be noted that the effective local Reynolds number, defined by

$$R_{\text{local}} = R_D b W_c \tag{19}$$

is a decreasing function of the axial distance as opposed to the two-dimensional case, where R_{local} remains practically constant. Therefore, a stronger viscous effect on the flowfield should be expected for an axisymmetric wake.

Calculations covering a range of Reynolds numbers are presented in Figs. 4–6. The effects of Reynolds number on the fluctuation are clearly displayed in Fig. 5. Both the rate of growth and the peak intensity of the fluctuation are reduced as the Reynolds number decreases. The corresponding effects on the centerline density defect ρ_c and the wake velocity W_c are shown in Figs. 4 and 6. The abscissa in these two plots have been normalized by the square root of Reynolds number. In this coordinate, the laminar steady solution is given by a single curve for all Reynolds numbers.

The mechanisms for the breakdown of a laminar wake have been fully discussed in Ref. 10 for a two-dimensional incompressible wake. The onset of transition occurs when the growing Reynolds stress term becomes comparable to the laminar viscous term. This picture is believed to remain intact with the introduction of compressibility. Since a lower Reynolds number means a larger laminar viscous contribution to the mean flow decay, therefore a larger amplitude must be reached before the Reynolds stress term becomes important. This effect, together with the lower rate of amplification for the fluctuation, results in a delay of "transition" as the Reynolds number decreases. For the smallest Reynolds number calculated ($R_D = 5 \times 10^4$), the fluctuation field has not been able to influence the mean field in any noticeable manner, and the flow is virtually laminar throughout.

So far, the term "transition" has been used somewhat loosely. In order to illustrate the dependence of the transition process on the edge Reynolds number in a more quantitative way, two arbitrary definitions of transition location are used, and the results are presented in Fig. 7. The broken line corresponds to the location where the fluctuation energy density $Z = 2 \times 10^{-4}$ (arbitrarily defined for the purpose of demonstrating a threshold in detectable signal), whereas the solid line gives the intersection of the maximum slope with the laminar steady solution on the W_c vs x/D plot. It may be noted that the numerical results cannot be correlated by a simple power law, such as $x_t/D \sim R_D^{-1}$. It is conceivable that a collection of data over a limited range of Reynolds number may lead to a specific power-law dependence. The nonexistence of transition location above certain altitude is also interesting to note.

3.1.4. *Mach number effect*

It is indicated in expression (15) that the eigenvalue and the eigenfunction are functions of the edge Mach number. Moreover, Mach number also appears explicitly in the integral conservation equations. Using the same initial conditions, (18), the transition location defined by the maximum slope intercept is also plotted for $M_e = 10$ on Fig. 7. The result confirms the stabilizing effect of increasing Mach number.

Because of the lack of detailed measurements in the transition region of an axisymmetric, compressible wake, no experimental result has been compared with the present calculations. Therefore, more quantitative justification of the approach will have to rely on rather idealized situations. The rather favorable comparison with the experiment of Sato and Kuriki has provided some justification of this gen-

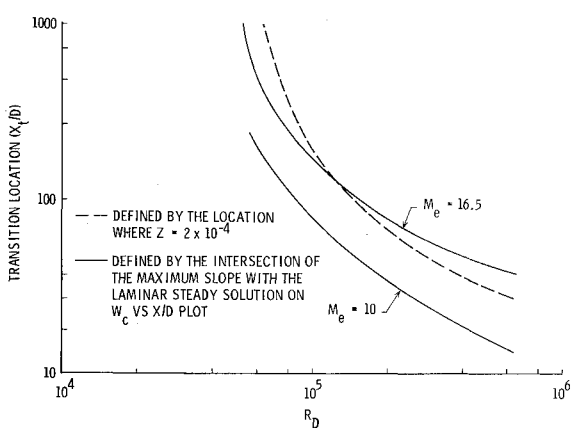

Fig. 7 Effects of Reynolds number and Mach number on the transition location.

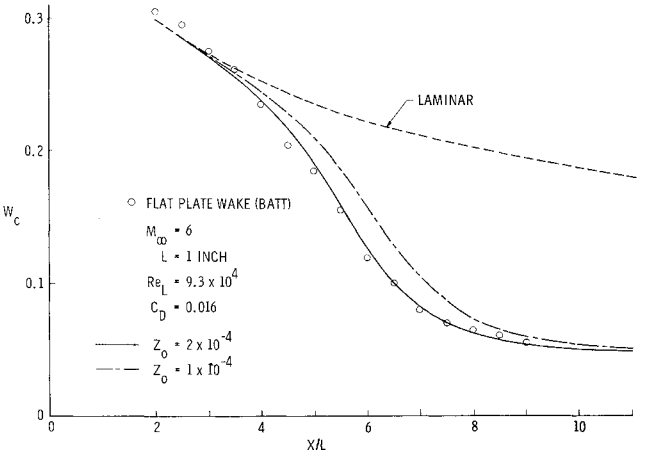

Fig. 8 Comparison of the centerline velocity defect for two-dimensional compressible wake.

eral approach. A test for the present compressibility modeling will have to come from the comparison with a two-dimensional, compressible wake to be discussed in the next section.

3.2. Two-Dimensional Compressible Wake

A large number of laboratory experiments for two-dimensional compressible wakes have been reported, including some detailed measurements in the transition region. For the purpose of comparison, calculations are carried out for the compressible wake behind a flat plate. The calculated results are then compared with the mean flow measurements of Batt[17] and the fluctuation field measurements of Behrens and Ko.[3] The specific flow conditions are

freestream Mach number, $M_\infty = 6$
Reynolds number based on L, $R_L = 9.3 \times 10^4$
averaged drag coefficient, $C_D = 0.016$

3.2.1. *Linear stability equations*

The linear stability theory has indicated that an antisymmetric fluctuation is more unstable than a symmetric one for two-dimensional flows. Thus, only antisymmetric two-dimensional disturbances are considered. The experimentally observed dominating frequency of 70 kHz, which corresponds to a nondimensional frequency $\omega = 13$, is chosen to be the characteristic mode.

3.2.2. *Comparison between theory and experiment*

The calculated velocity and density defects are compared with the measurements of Batt in Figs. 8 and 9. Two sets of solution curves corresponding to two different initial levels of turbulent intensity Z_0 are shown in each figure, together with the laminar solution. A good agreement of the velocity defect W_c throughout the measured region is obtained for $Z_0 = 2 \times 10^{-4}$. However, a better agreement with the experimentally determined density defect ρ_c is seen for $Z_0 = 1 \times 10^{-4}$. Since the solution curves are nearly translated in the axial direction by changing the magnitude of Z_0, the choice of such a value needs some justifications. This justification is partially given by the comparison of the calculated fluctuation energy with the measurements of Behrens and Ko for the same model in Fig. 10. Since the experimental hot-wire data were not reduced, a direct quantitative comparison with the calculation was not possible. However, a sensible comparison can be made by normalizing the data with the initial magnitude at station $x/L = 2$. Figure 10 shows a reasonably good agreement for the calculation obtained by setting $Z_0 = 2 \times 10^{-4}$, especially in the peak magnitude. A change of Z_0 by a factor of 2 causes a relatively small change in the solution curves for W_c and ρ_c, as

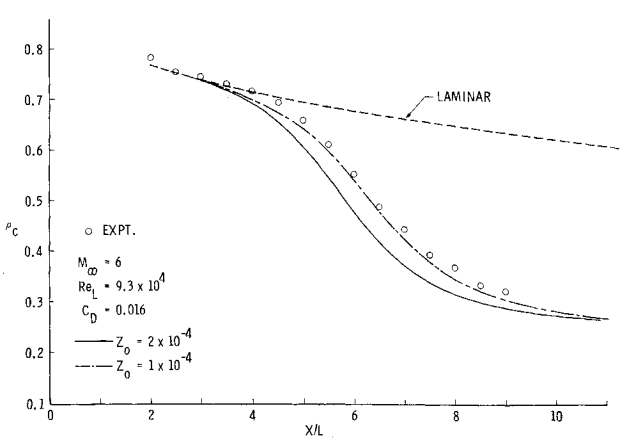

Fig. 9 Comparison of the centerline density defect for two-dimensional compressible wake.

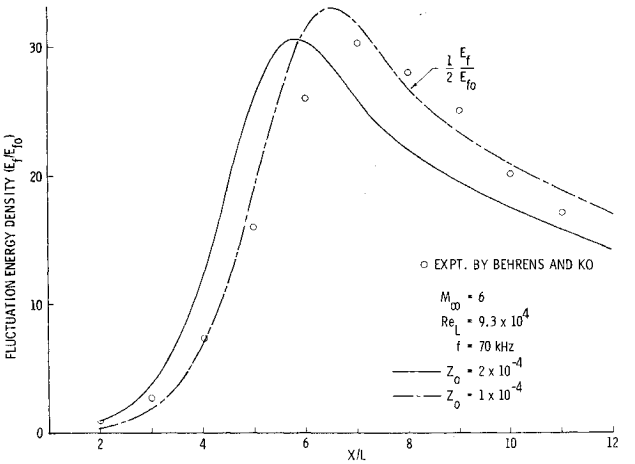

Fig. 10 Comparison of the fluctuation energy ratio for two-dimensional compressible wake.

indicated in Figs. 8 and 9. However, the change in Z is much more dramatic. It should be noted that the solution for $Z_0 = 1 \times 10^{-4}$ is plotted in half-scale in Fig. 10. These results clearly indicate that the ratio of the peak turbulent intensity to an initial reference station is the most sensitive result with respect to the change in initial conditions and can be used as an indicator for the correct initial values. It should also be noted that $Z_0 = 2 \times 10^{-4}$ corresponds to 1.5% velocity fluctuation. The freestream turbulence level in the GALCIT hypersonic wind tunnel where the test was conducted has been determined to be between $\frac{1}{4}$ and $\frac{1}{2}$%. Therefore, this level of initial fluctuation intensity at $x/L = 2$ is quite acceptable when certain growth in magnitude before $x/L = 2$ is taken into account.

IV. Conclusion

The stability-oriented integral approach has been successfully applied to the study of the laminar-turbulent transition of the axisymmetric as well as the two-dimensional wakes. Favorable comparison with the experiments of Batt and Behrens and Ko for a two-dimensional wake at $M_\infty = 6$ tends to substantiate the theoretical model. Any quantitative comparison of the axisymmetric case was hampered by the lack of detailed measurements in the transition region. Some well controlled experiments in axisymmetric wake are needed to give a better assessment of the theory.

The outer inviscid wake has been completely neglected in the present analysis. Modifications to include the outer inviscid wake should be incorporated into the present theory in order to treat bodies of relatively blunted nose.

References

[1] Sato, H. and Kuriki, K., "The Mechanism of Transition in the Wake of a Thin Flat Plate Placed Parallel to a Uniform Flow," *Journal of Fluid Mechanics*, Vol. 2, 1961, pp. 321–352.

[2] Sato, H. and Okada, O., "The Stability and Transition of an Axisymmetric Wake," *Journal of Fluid Mechanics*, Vol. 26, Pt. 2, 1966, pp. 237–253.

[3] Behrens, W. and Ko, D. R. S., "Experimental Stability Studies in Wakes of Two-Dimensional Slender Bodies at Hypersonic Speeds," *AIAA Journal*, Vol. 9, No. 5, May 1971, pp. 851–857.

[4] Stuart, J. T., "On the Non-Linear Mechanics of Wave Disturbances in Stable and Unstable Parallel Flows. Part 1. The Basic Behavior in Plane Poiseuille Flow," *Journal of Fluid Mechanics*, Vol. 9, 1960, pp. 353–370.

[5] Watson, J., "On the Non-Linear Mechanics of Wave Disturbances in Stable and Unstable Parallel Flows. Part 2. The Development of a Solution for Plane Poiseuille Flow and for Plane Couette Flow," *Journal of Fluid Mechanics*, Vol. 9, 1960, pp. 371–389.

[6] Watson, J., "On Spatially-Growing Finite Disturbances in Plane Poiseuille Flow," *Journal of Fluid Mechanics*, Vol. 14, 1962, pp. 211–221.

[7] Taylor, G. I., "Stability of a Viscous Liquid Contained Between Two Rotating Cylinders," *Philosophical Transactions of the Royal Society*, Vol. A223, 1923, pp. 289–343.

[8] Liu, J. T. C., "A General Theory of the Development of Finite-Amplitude Disturbances in the Unstable Laminar Wake Behind Plane Bodies at Hypersonic Speeds," AIAA Paper 68-684, Los Angeles, Calif., 1968.

[9] Ko, D. R. S., "Non-Linear Stability Theory for a Laminar, Incompressible Wake," Part II, Ph.D. thesis, 1969, California Inst. of Technology.

[10] Ko, D. R. S., Kubota, T., and Lees, L., "Finite Disturbance Effect on the Stability of a Laminar Incompressible Wake Behind a Flat Plate," *Journal of Fluid Mechanics*, Vol. 40, Pt. 2, 1970, pp. 315–341.

[11] Lin, C. C., "On Uniformly Valid Asymptotic Solutions of the Orr-Sommerfeld Equation," *Proceedings of the 9th International Congress of Applied Mechanics*, 1957, pp. 136–148.

[12] Lees, L. and Gold, H., "Stability of Laminar Boundary Layers and Wakes at Hypersonic Speeds. Part I. Stability of Laminar Wakes," *Proceedings of International Symposium of Fundamental Phenomena in Hypersonic Flow*, Cornell University Press, Ithaca, N.Y., 1966.

[13] Batchelor, G. K. and Gill, A. E., "Analysis of the Stability of Axisymmetric Jets," *Journal of Fluid Mechanics*, Vol. 14, 1962, pp. 529–551.

[14] Mack, L. M., "Computation of the Stability of the Laminar Boundary Layer," *Methods in Computational Physics*, Vol. 4, Academic Press, New York, 1965, pp. 247–299.

[15] Lees, L. and Hromas, L. A., "Turbulent Diffusion in the Wake of a Blunt-Nosed Body at Hypersonic Speeds," *Journal of the Aerospace Sciences*, Vol. 29, No. 8, Aug. 1962.

[16] Ohrenberger, J. T. and Baum, E., "A Theoretical Model of the Near Wake of a Slender Body in Supersonic Flow," AIAA Paper 70-792, Los Angeles, Calif., 1970.

[17] Batt, R. G., "Experimental Investigation of Wakes Behind Two-Dimensional Slender Bodies at $M = 6$," Ph.D. thesis, 1967, California Inst. of Technology.

SEPTEMBER 1971 AIAA JOURNAL VOL. 9, NO. 9

Aerodynamics of Slender Bodies and Wing-Body Combinations at $M_\infty = 1$

JOHN R. SPREITER*
Stanford University, Stanford, Calif.

AND

STEPHEN S. STAHARA†
Nielsen Engineering & Research Inc., Mountain View, Calif.

An account is given of recent theoretical results for steady inviscid transonic flows around a variety of three-dimensional bodies of aerodynamic interest. The local linearization method for axisymmetric flow is combined with the transonic equivalence rule to calculate pressure distributions for freestream Mach number one on the surface and in the near flowfield of a number of slender, pointed, axisymmetric and nonaxisymmetric bodies, including simple wing-body combinations, for both nonlifting and lifting conditions. Comparisons with experiment exhibit good agreement, except near the rear of some of the bodies, particularly those with maximum thickness far forward or on lifting bodies at larger angles of attack. It is suggested that the former is due primarily to wind-tunnel wall interference, and the latter to boundary-layer separation and vortex generation.

I. Introduction

THE purpose of this paper is to describe a theoretical procedure for determining the pressure distributions at freestream Mach number M_∞ equal unity on the surface and in the near flowfield of slender bodies and wing-body combinations, both nonlifting and lifting, and to demonstrate the quality of the results by comparison with experiment. The analysis is based on the small disturbance theory of inviscid transonic flow, and makes use of the approximations of slender-body theory, the transonic equivalence rule, and the method of local linearization for axisymmetric flow with $M_\infty = 1$. Results are presented for bodies of revolution having maximum diameter located between 30% and 70% of the body length, for parabolic-arc bodies of elliptic cross section, and for both a conical and a more general wing-body combination. Angles of attack α range from 0° to 6°. The examples were selected, insofar as possible, to enable comparison with existing data obtained either in a conventional transonic wind tunnel with partly open walls or in a solid-wall wind tunnel operating in the choked condition to simulate flow with $M_\infty = 1$.

Received June 15, 1970; presented as Paper 70-798 at the AIAA 3rd Fluid and Plasma Dynamics Conference, Los Angeles, Calif., June 29–July 1, 1970; revision received December 17, 1970. This work was supported by NASA/Ames Research Center under Contract NAS2-5410.

* Professor, Departments of Applied Mechanics and Aeronautics and Astronautics; also Consultant, Nielsen Engineering & Research Inc. Associate Fellow AIAA.

† Senior Research Scientist. Member AIAA.

II. Theory

Basic Equations

The analysis is expressed primarily in terms of a body-fixed Cartesian coordinate system centered at the nose with the x axis directed rearward and aligned with the longitudinal axis of the body, the y axis directed to the right, facing forward, and the z axis directed vertically upward, as illustrated in Fig. 1. The freestream direction may be inclined any small